Dispersion of Traffic Exhausts in Urban Street Canyons with Tree Plantings - Experimental and Numerical Investigations -

C. Gromke[1], J. Denev[2], B. Ruck[1]

[1]Laboratory of Building- and Environmental Aerodynamics, Institute for Hydromechanics
[2]Institute for Chemical Technology
University of Karlsruhe
Karlsruhe, Germany
gromke@ifh.uka.de

Abstract - Wind tunnel experiments and numerical computations have been performed in order to investigate the influence of avenue-like tree plantings on the dispersion of traffic exhaust in an urban street canyon. Reduced natural ventilation and enhanced pollutant concentrations have been found in the presence of trees. A comparison of experimental and numerical results shows qualitative good, but quantitative rather poor agreement. In the numerical computations, flow velocities are underestimated and pollutant concentrations are overestimated.

Key words - trees, pollutant dispersion, urban street canyon, urban air quality, traffic exhausts

1 Introduction

The emission of traffic exhausts is one of the major sources for airborne pollutants in urban areas. In particular, narrow urban street canyons with large traffic volume are subject to high pollutant concentrations. Thus, it is important for the healthiness of inhabitants that sufficient natural ventilation is ensured which dilutes and removes the traffic emissions. A large number of studies have been devoted to pollutant dispersion processes in urban street canyons in the past, however, all of them were restricted to empty, obstacle-free street canyons (Chang and Meroney, 2003; Gerdes and Olivari, 1999; Kastner-Klein et al., 2001; Pavageau and Schatzmann, 1999). By contrast, the central question of the present investigation is, to what extent avenue-like tree plantings in urban street canyons influence the natural ventilation.

2 Approach

In order to clarify the influence of tree plantings on the dispersion of traffic exhausts, wind tunnel experiments at a small-scale urban street canyon model have been performed. Velocity and concentration measurements for an approaching boundary layer flow perpendicular to the canyon center axis have been carried out for different tree planting configurations. In the present article, emphasis is placed on variations of the crown permeability.

For further variations of characteristic tree planting parameters, e.g. tree spacing, crown shape and size or leaf free stem height, see Gromke and Ruck, 2006; Gromke and Ruck, 2007a; b; c; d. Furthermore, for the purpose of comparison, numerical investigations with a commercial CFD-code using a LVEL k-ε turbulence closure scheme have been performed and will be discussed.

3 Experimental Model Setup, Measurement Instrumentation and Numerical Model

The wind tunnel model (scale 1:150) consists of two parallel aligned rows of houses forming an isolated urban street canyon with aspect ratios H/W = 1 and L/H = 10 (Figure 1). Model tree arrangements with different crown porosities have been placed in one row along the street center axis. This arrangement was subjected to a boundary layer flow with profile exponent α = 0.30 according to the power law (Figure 9), approaching perpendicular to the street axis (Gromke and Ruck, 2005). The Reynolds number Re, calculated with the building height H and the velocity u(H) of the undisturbed flow at building height H, amounts to Re = 37000 and ensures a Reynolds-Number independent flow field.

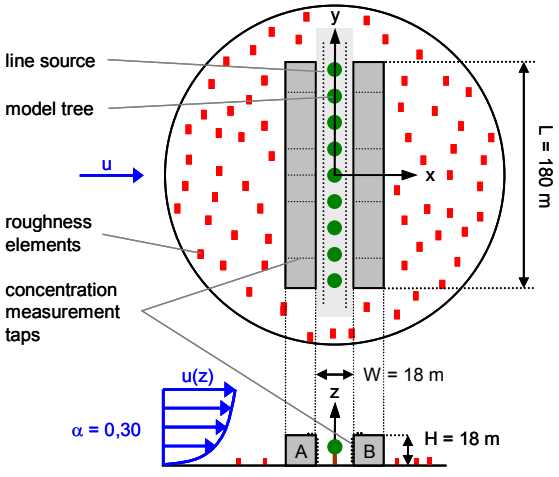

Figure 1. Model setup of street canyon (scale 1:150)

In-between the houses, a tracer gas emitting line source is embedded at street level for simulating the release of traffic exhausts (Meroney et al., 1996). Sulfur hexafluoride (SF_6) was used as tracer gas to model the traffic emissions. Measurement taps were applied along the inward canyon walls to sample the near-wall canyon air. These samples were analyzed by an Electron

Capture Detector (ECD) yielding mean concentrations. Laser-Doppler-Velocimetry (LDV) was used to measure flow velocities in the street canyon and to determine the rates of vertical air exchange between street canyon and atmospheric flow at roof top level.

The numerical computations have been performed by using the commercial CFD-code FLOVENT. This software package offers a LVEL k-ε turbulence model to close the Reynolds-Averaged-Navier-Stokes (RANS) equations. In near-wall regions, the turbulent viscosity ν_t is determined by a blending of the turbulent viscosity $\nu_{t,k\text{-}\varepsilon}$, calculated by the classical k-ε approach, and the turbulent viscosity $\nu_{t,LVEL}$, calculated by an algebraic LVEL approach using a characteristic length and velocity scale. Furthermore, wall functions for the treatment of wall-adjacent cells are included. The governing equations are numerically solved on a structured, staggered grid, using the finite volume method. Underlying discretization schemes are first order upwind and second order central differences for convection and diffusion terms, respectively. The turbulent Schmidt number Sc_t in the advection-diffusion equation is 1 and can not be varied (FLOVENT 6.1, 2005).

4 Measurement Results

4.1 Reference Case - Tree-free Street Canyon

Before presenting and discussing the measurement results obtained at street canyons with avenue-like tree plantings, the flow- and concentration field at the tree-free (so called reference) canyon, will be illustrated. In Figure 2, a schematic sketch of the flow field at the reference canyon is shown.

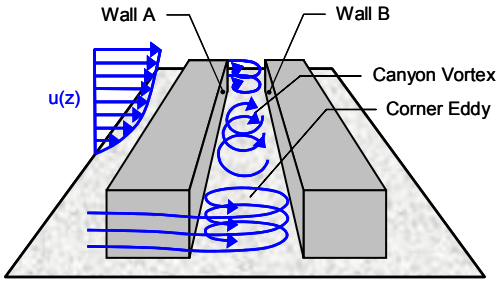

Figure 2. Flow field at empty street canyon (reference case)

Two essential vortex structures can be identified. The canyon vortex in the middle section of the street canyon and the corner eddies at the outer parts of the canyon. Driven by the atmospheric flow skimming over the roof top level, the canyon vortex is serving for vertical air exchange and thus providing pollutant dilution and removal in the middle section of the street canyon. Due to the corner eddies at the street ends, ambient air is entering the street canyon horizontally and serving for ventilation, too. At the street canyon ends, a superposition of both vortex structures takes place. According to Hunter et al., 1990/91, only in the middle section of long street canyons with aspect ratio L/H > 7, a distinct region with the canyon vortex being the solely dominating vortex structure can be observed.

In Figure 3, the normalized pollutant concentrations at the inward canyon walls are shown. These concentrations have been made dimensionless according to the formula

$$c^+ = \frac{c_{meas}\, L_{ref}\, u_{ref}}{Q_T / l} \qquad [-] \qquad (1)$$

with c_{meas} measured concentration, L_{ref} reference length characterizing a building dimension (L_{ref} = H), u_{ref} reference velocity characterizing the atmospheric flow (u_{ref} = u_H) and Q_T/l tracer gas source strength per unit length of the line source. Furthermore, the lengths have been normalized by the reference length L_{ref} = H.

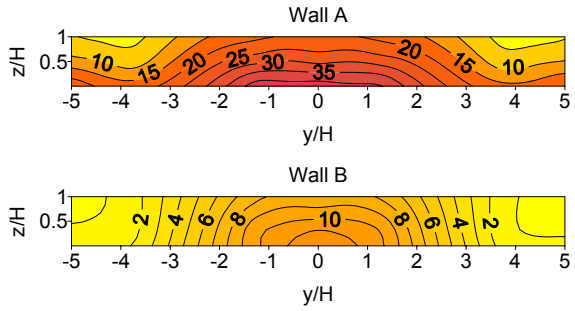

Figure 3. Normalized pollutant concentration c^+ [-] at canyon walls for reference case

Two characteristics of the concentration distribution at the inward canyon walls can be seen at once. First, the decline in concentration towards the street ends at both walls A and B, and second the much higher pollutant concentrations at wall A. The first characteristic is due to the superposition of the two different vortex structures at the street ends, providing enhanced ventilation. The second observation can be explained by following the canyon vortex for one rotation. At the roof top, an exchange between street canyon air and the skimming atmospheric flow takes place. Unpolluted air of the atmospheric flow is entrained into the rotating canyon vortex, which moves downwards into the street canyon in front of wall B. On the reverse flow from wall B towards wall A, released traffic exhausts near the bottom are getting accumulated in the canyon vortex. The upward motion of the vortex carrying the pollutants leads to high concentrations in front of wall A.

This is confirmed by the results of LDV measurements in a vertical cross section at y/H = 0.5. Figure 4 shows the normalized mean vertical velocity $w^+ = w/u_{ref}$ of the rotating canyon vortex measured in the reference canyon without trees. Ascending air flow in front of wall A and descending air flow in front of wall B are clearly visible. The maximum vertical velocity in the canyon vortex amounts to 25 % of the flow velocity at building height H.

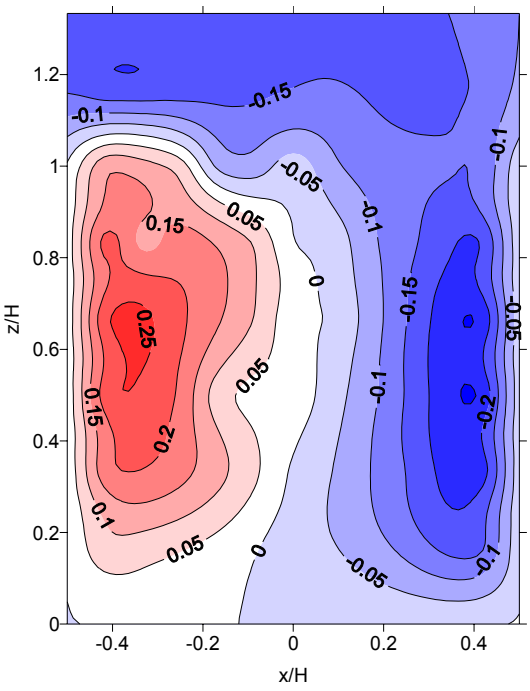

Figure 4. Normalized mean vertical velocity w^+ [-] between buildings at y/H = 0.5 for reference case

4.2 Continuous Tree Planting with impermeable Crown of rectangular Cross Section

The relative change in pollutant concentration at the canyon walls in the presence of a continuous tree planting with block shaped cross section of 9 m x 12 m when compared to the reference case (Figure 3) is presented in Figure 5. This configuration represents an avenue-like tree planting with a leaf-free stem height of 6 m and crowns interfering with each other, which is common for the urban environment. In this example, the crown permeability was neglected and Styrofoam was used to model the trees.

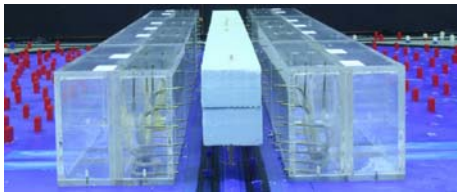

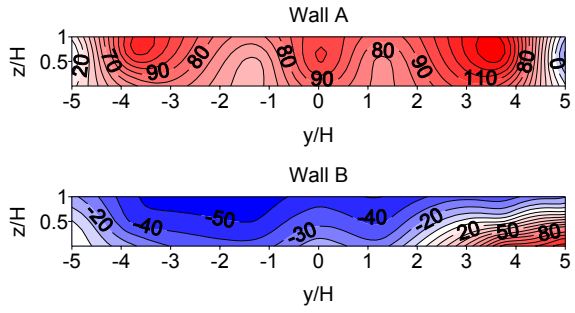

Figure 5. Relative change in pollutant concentration [%] for street canyon with impermeable, continuous crown of cross section 9 m x 12 m when compared to reference case (Figure 3)

At the leeward wall A, high increases in concentration are evident. Three pronounced areas of increases are evident. One is in the center part of the street canyon at y/H = 0 and the others at the canyon outer parts at ± 2.5 < y/H < ± 4. The high relative increases at the canyon outer parts are easy to explain. Due to the tree crowns, the corner eddies are effectively hindered in entering the street canyon laterally. Thus, one vortex structure which was serving for ventilation in the outer regions of the tree-free street canyon is missing or at least significantly reduced in strength. Comparing the flow fields in front of wall A at y/H = 0.5 in Figure 4 and Figure 6 reveals that the maximum velocity w^+ is only slightly smaller in the presence of the tree planting. However, because of the limited passage width, the volume flow rate of the remaining canyon vortex is reduced significantly. Consequently, the upward streaming flow in front of wall A contains higher concentrations of pollutants.

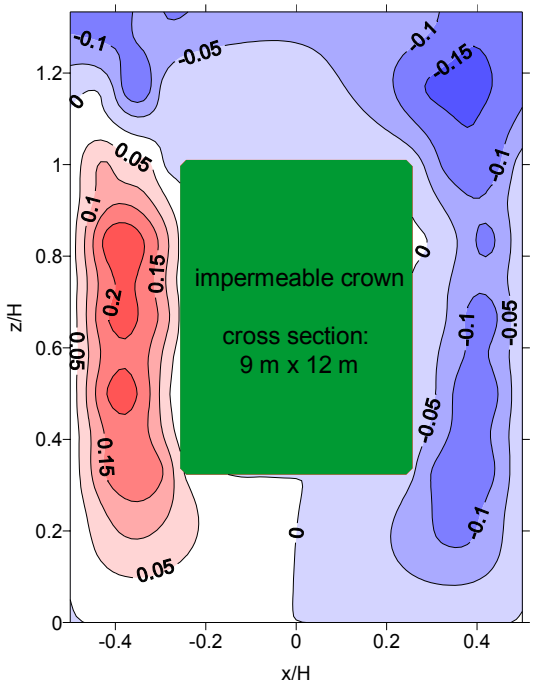

Figure 6. Normalized mean vertical velocity w^+ [-] between buildings at y/H = 0.5

At the windward wall B, decreases in concentration are visible (Figure 5). Considering the velocity plots of Figure 4 and Figure 6 shows modified flow fields at the roof top level. The upward moving stream in front of wall A extends farther into the skimming atmospheric flow in the case of the street canyon with tree planting. This means that the polluted air is discharged into higher layers of the above roof wind and is thus better diluted. In addition, analyses of the fluctuating part of the vertical velocity (not shown here) show enhanced turbulence intensities in the presence of the tree planting. The air which is entrained into the canyon in front of wall B is less polluted, leading to the smaller concentrations observed.

4.3 Continuous Tree Planting with permeable Crown of rectangular Cross Section

Now, the relative change in pollutant concentration for the same street canyon arrangement as addressed before, but with a permeable instead an impermeable crown is discussed. In order to take the crown porosity and permeability into account, an open-pored foam material (foam ppi 10) with a volume porosity of 97 % and a pressure loss coefficient λ = 250 Pa (Pa m)$^{-1}$ was used to model the trees. Figure 7 shows the relative change in concentration when compared to the reference case (Figure 3), (top) and when compared to the impermeable crown arrangement, (bottom).

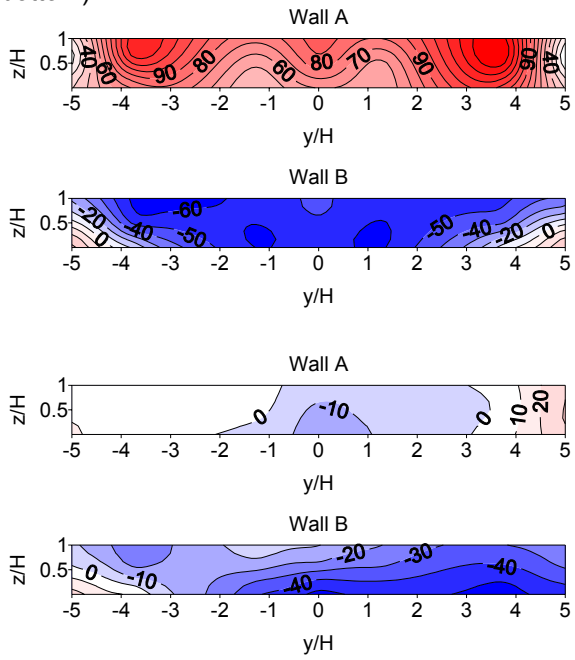

Figure 7: Relative change in pollutant concentration [%] for street canyon with permeable, continuous crown of cross section 9 m x 12 m when compared to reference case (Figure 3), (top) and relative change in pollutant concentration [%] when compared to impermeable crown, (bottom).

The typical characteristics of the concentration distribution known from the impermeable crown arrangement with increased concentrations at the leeward wall A and decreased concentrations at the windward wall B are found (Figure 7 top). A direct comparison of the two setups reveals only minor relative differences at wall A and moderate relative differences at wall B (Figure 7 bottom). The effect of crown permeability is of secondary importance for the pollutant concentrations at the canyon walls. At wall A, the relative average change in concentration amounts to - 3 % and at wall B to - 31 %. The absolute changes in concentrations at wall B are small, too. However, due to intrinsic lower concentrations at this wall (Figure 3), the relative changes appear to be enhanced when compared to wall A. Considering the flow fields for the impermeable and permeable crown arrangements in Figure 6 and Figure 8, reveals only negligible deviations in the mean vertical velocity component w^+.

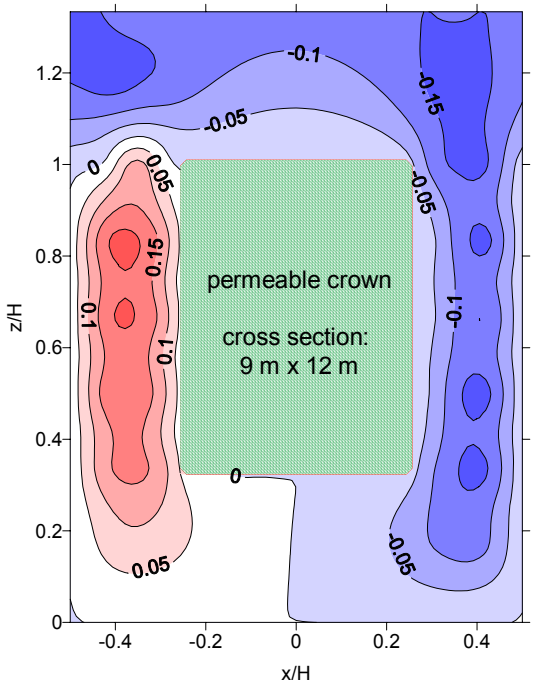

Figure 8. Normalized mean vertical velocity w^+ [-] between buildings at y/H = 0.

5 Numerical Results

The first step in numerical modeling was to generate the approaching flow and boundary conditions of the wind tunnel experiments (Gromke and Ruck, 2005). Figure 9 shows the computed and measured vertical profiles of mean flow and turbulence intensity profiles u(z) and I_{xyz}(z) at the origin of the co-ordinate system (Figure 1) for the empty domain. The agreement between experimental and numerical data is quite satisfactory.

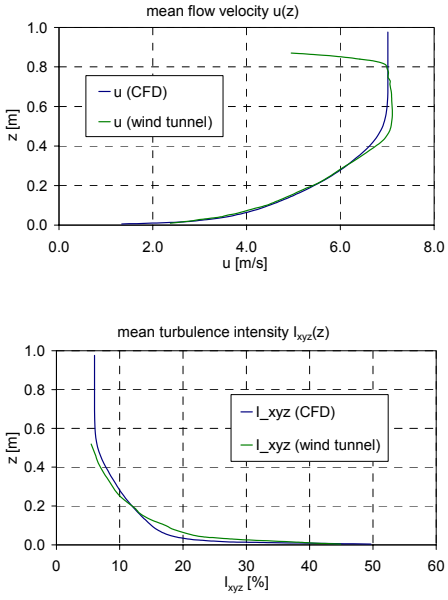

Figure 9. Vertical profiles of mean flow velocity u(z) [m/s] and mean turbulence intensity I_{xyz}(z) [%]

5.1 Reference Case - Tree-free Street Canyon

The next step was to model the reference case, i.e. the empty, tree-free street canyon. One of the well-know deficiencies of k-ε turbulence models is the stagnation point anomaly. This anomaly leads to overstated pressure values around the stagnation point at the building's windward face. Furthermore, an excessive production of turbulent kinetic energy k is predicted at the building's leading roof edge. The overestimation of k causes an enhanced transport of momentum from higher layers downward to the roof. This net downward momentum flux reduces the separation bubble or even suppresses the separation of the flow at the leading roof edge. However, since separation phenomena are important for the flow field and the pollutant dispersion in the wake of the building, i.e. in the street canyon, some effort was made to generate the flow separation at the leading edge.

LDV measurements of the mean flow around the windward building A and above the street canyon at roof top level at y/H = 0.5 are shown in Figure 10. The model buildings are made of Perspex and have a very smooth surface. As expected, the characteristic eddy at the bottom in front of the building and the separation bubble at roof level can be seen clearly (Figure 10 top). In the vector plot showing the flow field at roof level above the street canyon (Figure 10 bottom), the upper part of the canyon vortex can be identified. As can be seen, the canyon vortex protrudes into the skimming atmospheric flow above the buildings.

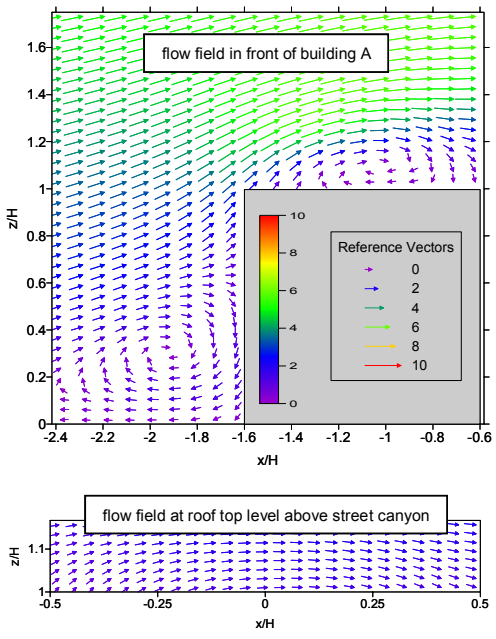

Figure 10. Vector plots of mean flow around windward building A and at roof top level above street canyon at y/H = 0.5 (LDV measurements)

As stated before, special attention was paid to generate flow separation at the windward edge of building A. Additionally to embedded refined grids around the street canyon arrangement, a grid refinement study was performed at the roof top and windward edge of building A. In a first attempt, numerical computations were performed without any special gird refinement (coarse grid) near the building walls. The resulting flow fields at the roof level above the windward edge of building A and the street canyon are shown in Figure 11.

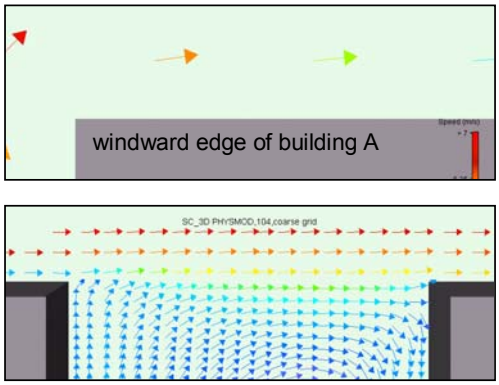

Figure 11. Vector plots of mean flow at roof level at y/H = 0.5 for coarse grid case

Neither flow separation at the windward edge nor a canyon vortex protruding into the skimming above roof flow can be seen. The canyon vortex remains completely inside the street canyon, suggesting a weak air exchange in the canyon's middle part.

In order to obtain flow separation at the leading edge, a refined grid was generated at the roof top level of building A. The corresponding flow fields above the windward building A and the street canyon are shown in Figure 12.

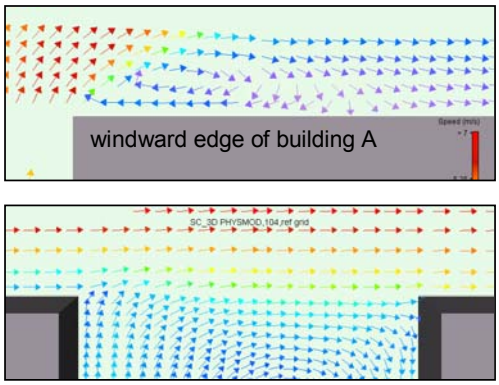

Figure 12. Vector plots of mean flow at roof level at y/H = 0.5 for refined grid case

This time, flow separation and a separation bubble above building A can be observed (Figure 12 top). Furthermore, regarding the upper street canyon flow field (Figure 12 bottom) reveals a canyon vortex protruding into the above-roof flow. Typical flow field characteristics as measured at the wind tunnel setup are evident.

The normalized pollutant concentrations at both canyon walls A and B for the coarse and refined grid are shown in Figure 13. A comparison to the measured pollutant concentrations (Figure 3) reveals considerably higher values in the case of the numerical computations, one reason for this is the

relatively high value of Sc_t = 1.0. In average, the numerically predicted concentrations at wall A are 1.9 times higher for the coarse grid case and 1.3 times higher for the refined grid case. The corresponding factors for wall B are 2.9 and 2.8, respectively. Concerning the general shape of the pollutant concentration distributions at the canyon walls, a better agreement with the measurements is found for the refined gird case with vertical concentration gradients in the middle part of wall A and horizontal gradients at wall B. Although the numerically predicted separation bubble and recirculation zone (Figure 12 top) are much smaller than experimentally measured (Figure 10 top), the concentration field inside the street canyon is highly sensitive to separation phenomena at the windward edge.

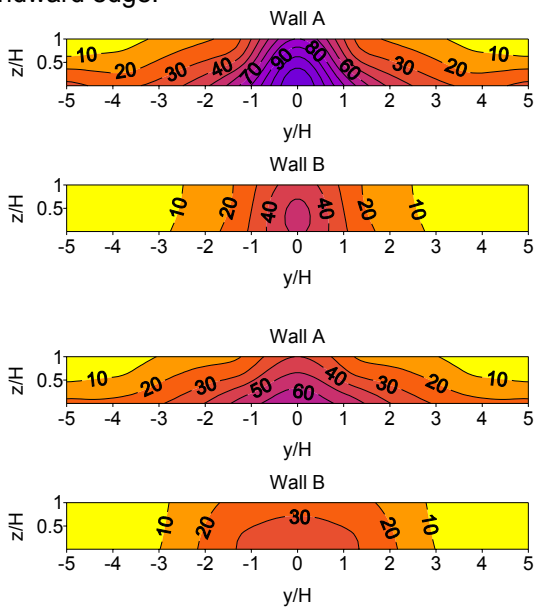

Figure 13. Normalized pollutant concentration c^+ [-] for reference case with coarse grid (top) and refined grid (bottom)

The contour plot of the normalized vertical velocity component w^+ inside the street canyon with refined grid at the roof level of windward building A is shown in Figure 14. In comparison to the LDV measurements of the wind tunnel experiment (Figure 4), the numerical computation results in significantly lower flow velocities. A reason for underestimating the velocity is the combination of first order upwind convection scheme with the present LVEL k-ε model. This means that the canyon vortex strength is weaker and less air is exchanged between canyon flow and atmospheric above-roof flow. Consequently, the pollutant concentrations, as predicted by the numerical computation, are higher. A comparison between the numerical results of the coarse and refined grid reveals similar vertical velocity fields, but slightly smaller flow velocities in the case of the coarse grid (not shown here). This is because of reduced momentum exchange between the skimming flow and the air masses below the roof top level, which is driving the canyon vortex (Figure 11 and Figure 12).

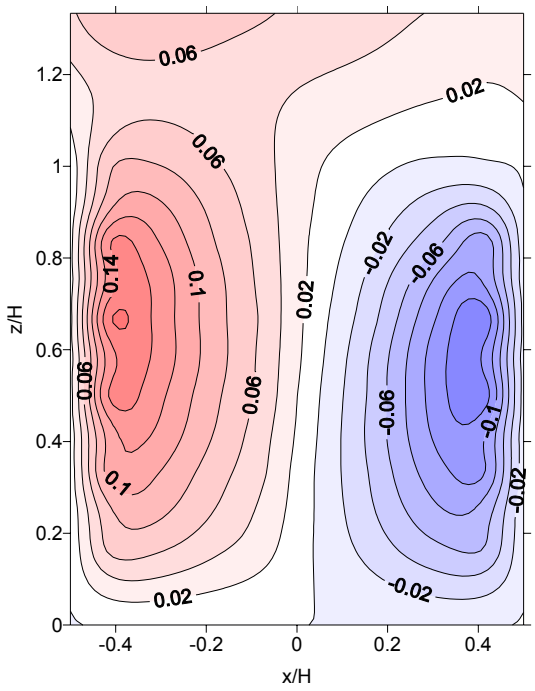

Figure 14. Normalized mean vertical velocity w^+ [-] at y/H = 0.5 for reference case with refined grid

5.2 Continuous Tree Planting with impermeable Crown of rectangular Cross Section

The tree planting already described and studied experimentally in chapter 4.2 has been investigated numerically, too. Since the wall average concentrations as well as the shape of the concentration distribution at the canyon walls show more similarity to the measurement results of Figure 3 for the refined grid case (Figure 13 bottom), the numerical computation was performed with the refined grid at the roof level of leeward building A. The relative change in concentrations when compared to the reference case (Figure 13 bottom) is shown in Figure 15.

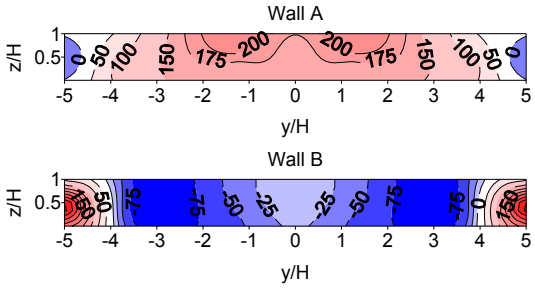

Figure 15. Relative change in pollutant concentration [%] for street canyon with impermeable, continuous crown of cross section 9 m x 12 m when compared to reference case (Figure 13 bottom)

Like in the experimental results (Figure 5), pronounced increases in concentration are visible at wall A. Whereas the increases in concentrations at the canyon's outer part at ± 3.5 < y/H < ± 4.5 are of same size, both in numerical and experimental results, the relative change in concentration at the canyon's middle part is significantly

higher in the numerical simulation. Furthermore, the decrease in concentration at y/H = ± 5 is stronger in the numerical results. At wall B decreases in concentration can be found in wide parts. However, at the middle part around y/H = 0, weaker concentration decreases are predicted, differing from the experimental results (Figure 5).

Figure 16 shows the contour plot of the normalized vertical velocity component w^+ inside the street canyon at y/H = 0.5. The magnitude of the updraft in front of the leeward wall A is comparable to the numerical reference case (Figure 14). However, in combination with the limited passage width due to the tree arrangement, the volume flow rate of the rotating canyon vortex is considerably reduced to 51 % of the volume flow rate of the numerical reference case. In front of wall B, a modified flow field is present. Contrary to the experimental results (Figure 6), a recirculation vortex develops in the gap between the tree crown and the windward wall B (Figure 17).

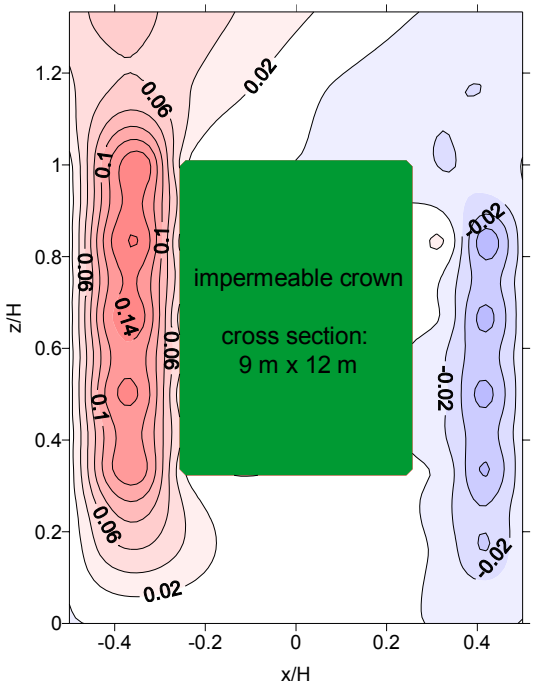

Figure 16. Normalized mean vertical velocity w^+ [-] between buildings at y/H = 0.5

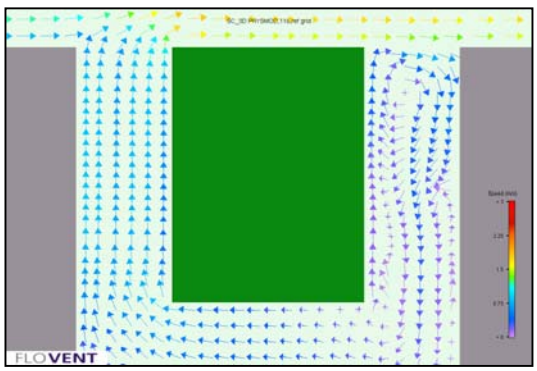

Figure 17. Vector plot of mean flow in street canyon with impermeable crown at y/H = 0.5

6 Summary

Flow and pollutant dispersion processes inside a typical urban street canyon with and without trees have been investigated. Avenue-like tree plantings consisting of crowns interfering with each other and forming a rectangular cross-sectioned continuous block have been considered. Wind tunnel experiments as well as numerical computations have been performed for single-row tree arrangements placed along the street center axis. Tree plantings with different crown permeabilities, covering 33 % of the street canyon volume have been investigated.

For all tree planting arrangements investigated, an increase in the overall pollutant concentration inside the street canyon was found when compared to the empty street canyon without trees (reference case). A more detailed analysis revealed increased pollutant concentrations at the leeward canyon wall of the upwind building and decreased pollutant concentrations at the windward canyon wall of the downwind building. High relative increases were found at the street ends towards the intersections. The entrainment conditions at the roof top level as well as at the sidewise end cross sections were considerable modified due to tree plantings.

Qualitatively, the CFD results are in agreement with the wind tunnel experiments. However, the quantitative agreement is limited. The numerical computations result in higher pollutant concentration levels and lower flow velocities inside the street canyon. Furthermore, the importance of flow separation at the windward edge of building A for the concentration field inside the street canyon was demonstrated by the CFD-simulations. As a result of the grid refinement study, the LVEL k-ε turbulence model together with the first-order upwind convection scheme predicts flow separation only in the case of a very fine grid near the windward edge of building A.

In Table 1 the normalized wall average concentrations of all configurations investigated are summarized. The values in the brackets denote the relative change in concentration when compared to the reference case with refined grid.

configuration	exp. result		num. result	
	wall A	wall B	wall A	wall B
ref. case (coarse grid)	19.6	5.4	37.3	15.9
ref. case (refined grid)			26.1	15.0
impermeable crown	33.5 (+71 %)	3.6 (-33 %)	67.1 (157%)	9.7 (-35 %)
permeable crown	32.6 (+66 %)	2.4 (-55 %)	-	-

Table 1. Normalized wall average concentrations c^+ [-], values in brackets denote relative change in concentration when compared to refined grid case

Figure 18 shows the profiles of the normalized mean vertical velocity component w^+ at height z/H = 0.7 in a vertical cross section at y/H = 0.5. The corresponding normalized integrated vertical volume flow rates V^+ per unit spanwise length are summarized in Table 2. When multiplying these values with the reference velocity u_{ref} and the reference length L_{ref} = H, the vertical volume flow rate per unit spanwise length in $m^2 s^{-1}$ is obtained.

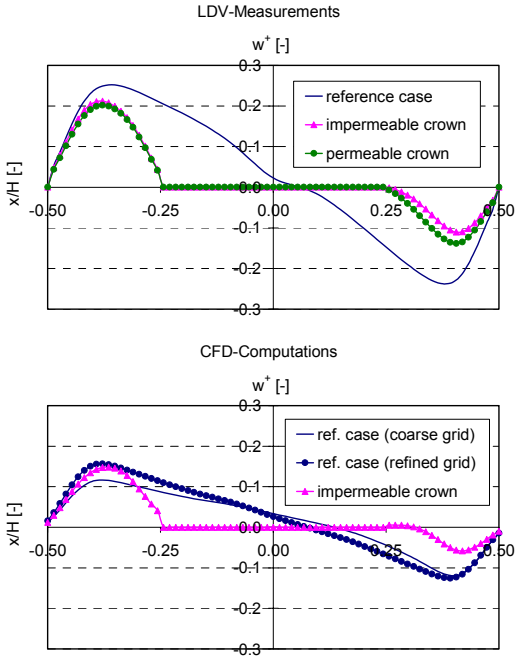

Figure 18. Normalized mean velocity w^+ [-] profiles at y/H = 0.5 and height of z/H = 0.7, experimental (top) and numerical (bottom) results

configuration	exp. result		num. result	
	wall A	wall B	wall A	wall B
ref. case (coarse grid)	0.082	-0.057	0.040	-0.023
ref. case (refined grid)			0.049	-0.029
impermeable crown	0.035 (-57 %)	-0.015 (-74 %)	0.025 (-49 %)	-0.006 (-79 %)
permeable crown	0.034 (-59 %)	-0.020 (-65 %)	-	-

Table 2. Normalized vertical volume flow rates V^+ [-] per unit spanwise length inside the street canyon at y/H = 0.5 and height z/H = 0.7, values in brackets denote relative change in volume flow rate when compared to refined grid case

Acknowledgement

The authors gratefully acknowledge the financial support of the Deutsche Forschungsgemeinschaft DFG, grant-no. Ru 345/28.

References

Chang, C. and Meroney, R.N., (2003). “Concentration and flow distributions in urban street canyons: wind tunnel and computational data”, *Journal of Wind Engineering and Industrial Aerodynamics, vol.* 91, pp. 1141 - 1154.

FLOVENT 6.1 (2005). “User’s Manuel”, *Flomerics Limited*, September 2005.

Gerdes, F. and Olivari, D., (1999). “Analysis of pollutant dispersion in an urban street canyon”, *Journal of Wind Engineering and Industrial Aerodynamics, vol.* 82, pp 105 - 124.

Gromke, C. and Ruck, B., (2005). “Die Simulation atmosphärischer Grenzschichten in Windkanälen“, *Proc. 13. GALA Fachtagung "Lasermethoden in der Strömungsmesstechnik",* Cottbus, September 2005, pp. 51-1 - 51-8.

Gromke, C. and Ruck, B., (2006). “Der Einfluss von Bäumen auf das Strömungs- und Konzentrationsfeld in Straßenschluchten“, *Proc. 14. GALA Fachtagung "Lasermethoden in der Strömungsmesstechnik"*, Braunschweig, September 2006, pp. 59-1 - 59-10.

Gromke, C. and Ruck, B., (2007a). “Influence of trees on the dispersion of pollutants in an urban street canyon - experimental investigation of the flow and concentration field”, *Atmospheric Environment*, vol. 41, pp. 3387 - 3302. http://dx.doi.org/10.1016/j.atmosenv.2006.12.043

Gromke, C. and Ruck, B., (2007b). “Trees in urban street canyons and their impact on the dispersion of automobile exhausts”, *Proc. 6th International Conference on Urban Air Quality*, Cyprus, March 2007.

Gromke, C. and Ruck, B., (2007c). “Flow and dispersion phenomena in urban street canyons in the presence of trees”, *Proc. 12th International Conference on Wind Engineering*, Australia, July 2007.

Gromke, C. and Ruck, B., (2007d). “Effects of trees on the dilution of vehicle exhaust emissions in urban street canyons”, *Special Issue on Urban Air Pollution in International Journal of Environment and Waste Management (IJEWM)*, paper accepted for publication, paper submitted on invitation.

Hunter, L.J., Watson, I.D. and Johnson, G.T., (1990/91). “Modelling air flow regimes in urban canyons”, *Energy and Buildings*, vol. 15, pp. 315 - 324.

Kastner-Klein, P., Fedorovich, E. and Rotach, M.W., (2001). “A wind tunnel study of organised and turbulent air motions in urban street canyons”, *Journal of Wind Engineering and Industrial Aerodynamics*, vol. 89, pp. 849 - 861.

Meroney, R.N., Pavageau, M., Rafailidis, S. and Schatzmann, M., (1996). “Study of line source characteristics for 2-D physical modelling of pollutant dispersion in street canyons”, *Journal of Wind Engineering and Industrial Aerodynamics*, vol. 62, pp. 37 - 56.

Pavageau, M. and Schatzmann, M., (1999). “Wind tunnel measurements of concentration fluctuations in an urban street canyon”, *Atmospheric Environment,* vol. 33, pp. 3961 - 3971.